Inorg. Chem. **2005**, *44*, 8087–8096

Cysteamine and Its Homoleptic Complexes with Group 12 Metal Ions. Differences in the Coordination Chemistry of Zn^{II}, Cd^{II}, and Hg^{II} with a Small N,S-Donor Ligand

Holger Fleischer,*,† Yvonne Dienes,†,§ Bernd Mathiasch,† Volker Schmitt,† and Dieter Schollmeyer‡

Institut für Anorganische Chemie und Analytische Chemie, Johannes Gutenberg Universität Mainz, Duesbergweg 10-14, D-55099 Mainz, Germany, and Institut für Organische Chemie, Johannes Gutenberg Universität Mainz, Duesbergweg 10-14, D-55099 Mainz, Germany

Received May 20, 2005

2-Ammoniumethanethiolate, $^{-}SCH_2CH_2NH_3^{+}$, the first structurally characterized zwitterionic ammoniumthiolate, is the stable form of cysteamine (HL) in the solid state and in aqueous solution. Reactions of $ZnCl_2$, $Cd(Oac)_2$, and $HgCl_2$ with cysteamine and NaOH in a 1:2:2 ratio, respectively, lead to the homoleptic complexes ML_2. Their single-crystal X-ray structures demonstrate basic differences in the coordination chemistry of Zn^{II}, Cd^{II}, and Hg^{II}. While chelating N,S-coordination modes are found for all metal ions, Zn^{II} forms a mononuclear complex with a distorted tetrahedral $Zn(N_2S_2)$ coordination mode, whereas Hg^{II} displays a dimer with $Hg(N_2S_2)$ coordinated monomers being connected by two long Hg···S contacts. Solid-state ^{199}Hg NMR spectra of HgL_2 and $[Hg(HL)_2]Cl_2$ reveal a low-field shift of the signals with increasing coordination number. Strong and nearly symmetric Cd–S–Cd bridges in solid CdL_2 lead to a chain structure, Cd^{II} displaying a distorted square pyramidal $Cd(N_2S_3)$ coordination mode. The ab initio [MP2/LANL2DZ(d,f)] structures of isolated ML_2 show a change from a distorted tetrahedral to bisphenoidal coordination mode in the sequence Zn^{II}–Cd^{II}–Hg^{II}. A natural bond orbital analysis showed a high ionic character for the M–S bonds and suggests that the S–M–S fragment is best described by a 3c4e bond. The strength of the M···N interactions and the stability of ML_2 toward decomposition to M and L–L decreases in the sequence Zn > Cd > Hg. Ab initio calculations further suggest that a tetrahedral S–M–S angle stabilizes Zn^{II} against substitution by Cd^{II} and Hg^{II} in a $M(N_2S_2)$ environment. Such geometry is provided in zinc-finger proteins, as was found by a database survey.

Introduction

Cysteamine, $H_2NCH_2CH_2SH$ (= HL), is a fundamental molecule which has an impact on various areas in chemistry. It ranks among the most important chelating ligands in coordination chemistry and preferably binds to soft metal ions. Numerous mononuclear,[1−3] as well as homo- and heterometallic oligonuclear complexes with a variety of coordination modes are known.[4−7] As the reactive part of coenzyme A, cysteamine is essential for biochemistry. It also allows the modeling of the binding of metals to peptides and proteins with cysteine and histidine donor sites.[8] Furthermore, cysteamine is of pharmaceutical use for the treatment of a disease called cystinosis.[9] Finally, it is of potential use for the synthesis of nanocrystalline semiconductors, for example, CdTe, since, like 2-mercaptoethanol, it is able to coordinate to the metal ions and stabilize small

* Author to whom correspondence should be addressed. E-mail: fleische@uni-mainz.de.

† Institut für Anorganische Chemie und Analytische Chemie.

‡ Institut für Organische Chemie.

§ Present address: Institut für Anorganische Chemie, RWTH Aachen University, Landoltweg 1, D-52074 Aachen, Germany.

(1) Stein, C.; Bouma, S.; Carlson, J.; Cornelius, C.; Maeda, J.; Weschler, C.; Deutsch, E.; Hodgson, K. O. *Inorg. Chem.* **1976**, *15*, 1183−1186.

(2) Briand, G. G.; Burford, N.; Cameron, T. S.; Kwiatkowski, W. *J. Am. Chem. Soc.* **1998**, *120*, 11374−11379.

(3) Konno, T.; Shimazaki, Y.; Kawai, M.; Hirotsu, M. *Inorg. Chem.* **2001**, *40*, 4250−4256.

(4) Wei, C. H.; Dahl, L. F. *Inorg. Chem.* **1970**, *9*, 1878−1887.

(5) Konno, T.; Chikamoto, Y.; Okamoto, K.; Yamaguchi, T.; Ito, T.; Hirotsu, M. *Angew. Chem., Int. Ed.* **2000**, *39*, 4098−4101.

(6) Yamada, Y.; Fujisawa, K.; Okamoto, K. *Bull. Chem. Soc. Jpn.* **2000**, *73*, 2067−2073.

(7) Konno, T. *Bull. Chem. Soc. Jpn.* **2004**, *77*, 627−649.

(8) Stillman, M. J.; Shaw, C. F., III; Suzuki, K. T. *Metallothioneins*; VCH Publishers: New York, 1992.

(9) Markello, T. C.; Bernardini, I. M.; Gahl, W. A. *New Eng. J. Med.* **1993**, *328*, 1157−1162.

10.1021/ic050814m CCC: $30.25
Published on Web 09/14/2005

Scheme 1. Structural Formulas of Compounds **1**−**4**

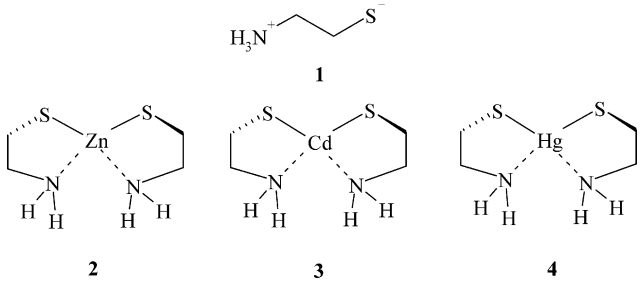

clusters.[10] Compared to its chemical significance, only little is known about the molecular structure of cysteamine.[11] The same applies to its complexes with d^{10} metal ions, where only a few have been structurally characterized so far.[2,12−15] The Zn^{2+} ion is known to have a high affinity toward nitrogen and sulfur donor ligands, as demonstrated by a considerable body of knowledge on Zn(N,S ligand) complexes.[14] The so-called structural zinc in biochemistry very often displays a $Zn(N_2S_2)$ coordination mode by binding to two cysteine and two histidine residues. This coordination mode is, for example, found in the zinc-finger proteins,[16] or liver alcohol dehydrogenase (LADH).[17,18] Part of the toxicity of the soft heavy-metal ions Pb^{2+}, Cd^{2+}, and Hg^{2+} is due to their competition with Zn^{2+} for binding to the cysteine and histidine sites. Complexes ML_2 (M = Pb, Zn, Cd, Hg; L = $-SCH_2CH_2NH_2$) should, hence, be suitable models of the $M(N_2S_2)$ coordination environment of these metals in enzymes. Complexes of Zn^{2+} and Pb^{2+} with cysteamine were recently reported.[13,15] The complex of Hg^{2+} with cysteamine hydrochloride, $[Hg(SCH_2CH_2NH_3)_2]Cl_2$, was published recently,[12] while the structure of HgL_2 was mentioned[19] but has not been published nor its data deposited yet. We, here, report results from single-crystal X-ray investigations, solution and solid-state NMR experiments, and ab initio quantum chemical studies of HL and the ML_2 complexes of Zn^{II}, Cd^{II}, and Hg^{II} (see Scheme 1).

Results and Discussion

Structure of 1 in the Solid State and in Solution. A survey of the melting points of the ethane derivatives XCH_2CH_2Y (X,Y = NH_2, OH, SH; Table 1) shows that cysteamine (X = NH_2; Y = SH) melts at significantly higher temperatures than the other compounds. In the solid state, cysteamine is present as 2-ammoniumthiolate, $^-SCH_2CH_2NH_3^+$, rather than 2-aminoethanethiol, $HSCH_2CH_2NH_2$ (Figure 1a and b), and it is the first structurally characterized zwitterionic ammoniumthiolate. In the noncentrosymmetric crystal, the molecules are associated via N−H···S hydrogen bonds in such a manner that each thiolate acts as a 3-fold acceptor and each ammonium group as a 3-fold donor (see Figure 1b). The resulting three-dimensional network of the molecules rationalizes the relatively high melting point of cysteamine. The type of hydrogen-bond network differs substantially from that in the cysteamine hydrochloride, $[HSCH_2CH_2NH_3]Cl$, where the $-NH_3$ and −SH groups donate and the Cl^- ions act as 4-fold accep-

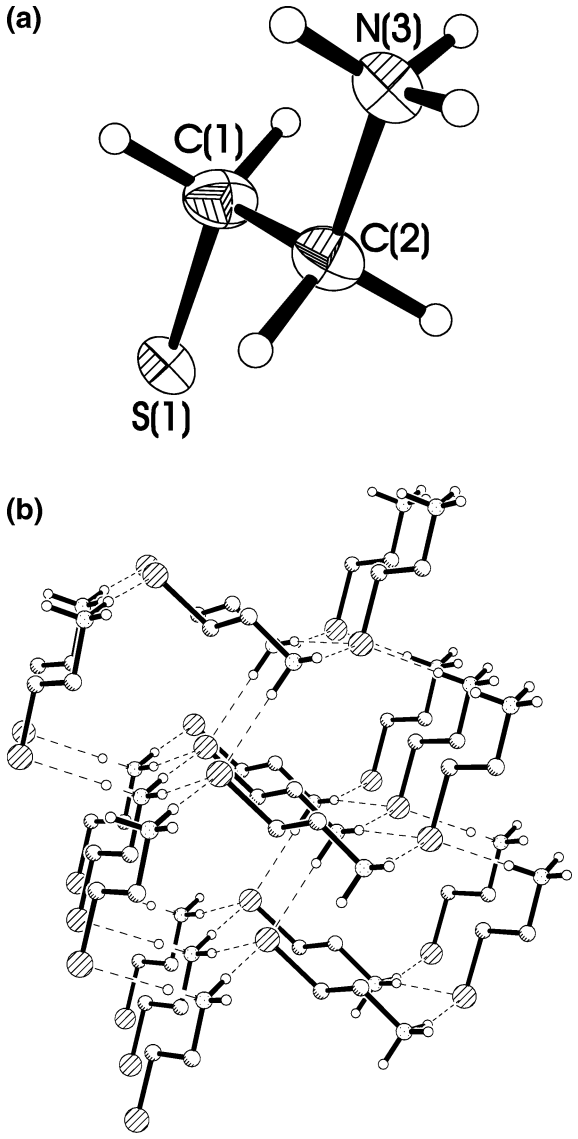

Figure 1. (a) ORTEP diagram of **1**. Displacement ellipsoids are at the 50% probability level. (b) Segment of the crystal structure of **1**. Hydrogen atoms bound to carbon atoms are omitted for clarity.

Table 1. Melting Points of Compounds XCH_2CH_2Y (X, Y = NH_2, OH, SH) in °C

	NH_2	OH	SH
NH_2	11[55]	10.5[56]	98−100[57]
OH		−13[58]	
SH			−41.2[59]

(10) Rockenberger, J.; Tröger, L.; Rogach, A. L.; Tischer, M.; Grundmann, M.; Eychmüller, A.; Weller, H. *J. Chem. Phys.* **1998**, *108*, 7808−7815.
(11) Barkowski, S. L.; Hedberg, K. J. *J. Am. Chem. Soc.* **1987**, *109*, 6989−6994.
(12) Kim, C.-H.; Parkin, S.; Bharara, M.; Atwood, D. *Polyhedron* **2002**, *21*, 225−228.
(13) Fleischer, H.; Schollmeyer, D. *Inorg. Chem.* **2004**, *43*, 5529−5536.
(14) Fleischer, H. *Coord. Chem. Rev.* **2005**, *249*, 799−827.
(15) Yamada, Y.; Miyashita, Y.; Fujisawa, K.; Okamoto, K. *Bull. Chem. Soc. Jpn.* **2001**, *74*, 97−98.
(16) Vallee, B. L.; Auld, D. S. *Acc. Chem. Res.* **1993**, *26*, 543−551.
(17) Eklund, H.; Nordström, B.; Zeppezauer, E.; Soderlund, G.; Ohlsson, I.; Bowie, T.; Soderberg, B. O.; Tapia, O.; Bränden, C. I. *J. Mol. Biol.* **1976**, *102*, 27−59.
(18) Makowska-Grzyska, M. M.; Jeppson, P. C.; Allred, R. A.; Arif, A. M.; Berreau, L. M. *Inorg. Chem.* **2002**, *41*, 4872−4887.
(19) Fleissner, G.; Kozlowski, P. M.; Vargek, M.; Bryson, J. W.; O'Halloran, T. V.; Spiro, T. G. *Inorg. Chem.* **1999**, *38*, 3523−3528.

tors.[20] Furthermore, the molecule exhibits an anti rather than a gauche conformation of the SCCN unit. It is, thus, different from the $[HSCH_2CH_2NH_3]^+$ cation present in the solid-state structure of cysteamine hydrochloride and also from the zwitterionic taurine, $^-O_3SCH_2CH_2NH_3^+$.[20,21]

Regarding the pK_a values of $[CH_3CH_2NH_3]^+$ (11.0, 25 °C),[22] $HSCH_2CH_3$ (11.26, 20 °C),[23] $[HOCH_2CH_2NH_3]^+$ (9.4, 25 °C),[24] and $HSCH_2CH_2OH$ (9.17, 25 °C),[25] the assignment of the two pK_a values of $[HSCH_2CH_2NH_3]^+$, 8.35 and 10.86,[26] to the SH and NH_3^+ groups, respectively, is not immediately evident. The titration of an aqueous solution of cysteamine hydrochloride with sodium hydroxide was monitored by ^{14}N NMR (H_2O/D_2O = 9:1) and Raman spectroscopy (H_2O only; Figure S1 in the Supporting Information). With no base added, a sharp peak was observed in the ^{14}N NMR spectrum at +29.9 ppm and the resonance at 2577 cm^{-1} in the Raman spectrum was attributed to the ν(S−H) mode. The addition of 1 equiv of NaOH to this solution did not affect the ^{14}N NMR signal, but the S−H band in the Raman spectrum disappeared. The addition of a further equivalent of NaOH led to a substantial broadening of the ^{14}N NMR signal and an upfield shift to +22.8 ppm. Obviously, the SH group is deprotonated prior to the NH_3^+ group. The changes in shift and shape of the ^{14}N NMR signal on addition of a second equivalent of NaOH are attributed to the deprotonation of the NH_3^+ group, causing a substantial reduction of the local symmetry at the N atom. Hence, cysteamine is present as the zwitterionic tautomer in aqueous solution as well.

Ab initio quantum chemical investigations should give a hint as to why cysteamine prefers the zwitterionic form in the solid state and in aqueous solution. Not very surprisingly, single-point energies of the isolated molecules show that the *anti*-$HSCH_2CH_2NH_2$ tautomer is thermodynamically stabilized against *anti*-$^-SCH_2CH_2NH_3^+$ (see Table 2; conformation refers to the C−C bond). The G2 energy of *gauche*-$HSCH_2CH_2NH_2$ is calculated to be 3 kJ mol^{-1} lower than that of the anti conformer, the small difference being attributed to an intramolecular S−H···N hydrogen bridge in the former. This is in accordance with findings for 2-(*N*,*N*-dimethylamino)ethanethiol.[27] Using an Onsager self-consistent reaction field in an aqueous solution (ϵ = 78.39), self-consistent reaction field (SCRF) HF/6-31G(d) geometry optimizations were performed, for *anti*-$HSCH_2CH_2NH_2$ and *anti*-$^-SCH_2CH_2NH_3^+$, followed by MP2/6-31G(d) single-point energy calculations (Table 2). Under these conditions, the zwitterionic form is thermodynamically favored over the nonzwitterionic form. Hence, the preference of the zwitterionic form in aqueous solution is mainly attributed to dipolar forces between the solute and the solvent.

Table 2. Selected Structural Data of **1** from Single-Crystal XRD, MP2/6-31G(d) Geometry Optimization of the Isolated Molecule and SCRF HF/6-31G(d) Geometry Optimization in an Aqueous Environment, and Energy Differences between $HSCH_2CH_2NH_2$ and $^-SCH_2CH_2NH_3^+$[a]

	XRD[b]	MP2[c]	SCRF[c,d]
S1−C1	1.823(3)	1.808	1.886
C1−C2	1.500(5)	1.498	1.546
C2−N3	1.487(4)	1.587	1.524
N3···S1#1	3.193(3)		
N3···S1#2	3.232(4)		
N3···S1#3	3.235(4)		
C2−C1−S1	111.6(2)	103.0	116.4
N3−C2−C1	109.5(3)	111.5	114.1
S1−C1−C2−N3	179.5(2)	180.0	180.0
N3−H3A···S1#1	177(5)		
N3−H3B···S1#2	172(4)		
N3−H3C···S1#3	164(5)		
ΔE[e]		204	−82

[a] Distances are given in Å, angles in degrees, and energies in kJ mol^{-1}. [b] Symmetry transformations used to generate equivalent atoms: #1 $x - 1/2$, $y + 1/2$, z; #2 $x - 1$, $-y + 1$, $z - 1/2$; #3 x, $-y + 1$, $z - 1/2$. [c] Anti conformation of $^-SCH_2CH_2NH_3^+$. [d] Self-consistent reaction field method according to Onsager. [e] $\Delta E = E(^-SCH_2CH_2NH_3^+) - E(HSCH_2CH_2NH_2)$. For details of the energy calculations, see text.

Crystal and Molecular Structures of 2−4. Complexes **2**−**4** (Scheme 1) were prepared according to the following reactions (Oac = acetate):

$$ZnCl_2 + 2NaOH + 2HL \rightarrow ZnL_2\ (\mathbf{2}) + 2NaCl + 2H_2O \quad (1a)$$

An attempt to synthesize **3** using $CdCl_2$ was not successful,

$$Cd(Oac)_2 + 2NaOH + 2HL \rightarrow CdL_2\ (\mathbf{3}) + 2NaOac + 2H_2O \quad (1b)$$

$$HgCl_2 + 2NaOH + 2HL \rightarrow HgL_2\ (\mathbf{4}) + 2NaCl + 2H_2O \quad (1c)$$

and CdCl(L) was obtained instead.[28] A coordination motif occurring in all three structures is the N,S-bidentate binding mode of $^-SCH_2CH_2NH_2$, leading to five-membered chelate rings. While one of the five-membered rings of **4** (Hg1−S2−C5−C6−N7) exists as a half chair, all others display envelope conformations. Apart from the common N,S-chelation, **2**, **3**, and **4** show rather different coordination modes at the metal, revealing basic differences in the coordination chemistry of Zn^{II}, Cd^{II}, and Hg^{II}.

Complex **2** exhibits a $Zn(N_2S_2)$ coordination mode, with CN_{Zn} = 4 and a distorted tetrahedral geometry around the metal (Figure 2a). Discrete C_2-symmetric molecules are linked via N−H···S hydrogen bonds, each NH_2 group being a 2-fold donor and each S atom a 2-fold acceptor (see Figure 2b). No intermolecular Zn···S contacts are present. The structural parameters describing the environment at Zn^{II} (Table 3) are very similar to those found for other complexes with a $Zn(N_2S_2)$ coordination mode.[14] The $Zn(SCH_2CH_2$-

(20) Kim, C.-H.; Parkin, S.; Bharara, M.; Atwood, D. *Polyhedron* **2002**, *21*, 225−228.
(21) Görbitz, A. H.; Prydz, K.; Ugland, S. *Acta Crystallogr., Sect. C* **2000**, *56*, e23−e24.
(22) Richard, J. T.; Toteva, M. M.; Crugeiras, J. *J. Am. Chem. Soc.* **2000**, *122*, 1664−1674.
(23) Bernasconi, A. F.; Killion, R., B.; Fassberg, J.; Rappoport, Z. *J. Am. Chem. Soc.* **1989**, *111*, 6862−6864.
(24) McCracken, P. G.; Ferguson, C. G.; Vizitiu, D.; Walkinshaw, C. G.; Wang, Y.; Thatcher, G. R. J. *J. Chem. Soc., Perkin Trans 2* **1999**, 911−912.
(25) Eldin, S.; Jencks, W. P. *J. Am. Chem. Soc.* **1995**, *117*, 4851−4857.
(26) Li, N. C.; Manning, R. A. *J. Am. Chem. Soc.* **1955**, *77*, 5225−5228.
(27) Ohno, K.; Matsumoto, S.; Aida, M.; Matsuura, H. *Chem. Lett.* **2003**, *32*, 828−829.
(28) Fleischer, H.; Schollmeyer, D. Manuscript in preparation.

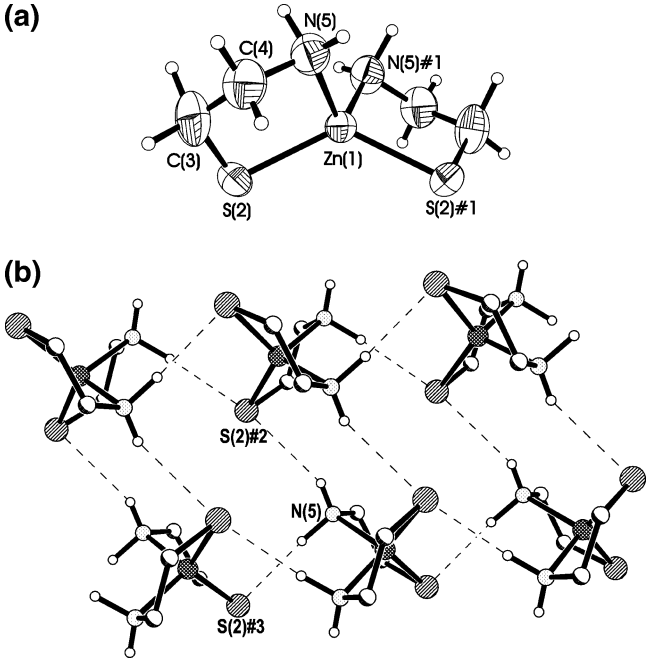

Figure 2. (a) ORTEP diagram of **2**. Displacement ellipsoids are at the 50% probability level. (b) Segment of the crystal structure of **2** showing intermolecular hydrogen bonds. Hydrogen atoms bound to carbon atoms are omitted for clarity.

Table 3. Selected Structural Data of **2** from Single Crystal XRD[a]

Zn1−S2	2.288(1)	S2−Zn1−S2#1	127.1(1)
Zn1−N5	2.054(3)	N5−Zn1−N5#1	107.8(2)
S2−C3	1.825(4)	Zn1−S2−C3	93.3(1)
C3−C4	1.486(6)	S2−C3−C4	115.1(3)
C4−N5	1.465(4)	C3−C4−N5	112.2(3)
N5···S2#2	3.474(3)	Zn1−S2−C3−C4	−27.9(3)
N5···S2#3	3.454(3)	S2−C3−C4−N5	50.8(5)
		C3−C4−N5−Zn1	−44.3(4)
		C4−N5−Zn1−S2	21.1(2)
		N5−Zn1−S2−C3	3.0(2)
		S2#1−Zn1−S2−C3	133.3(2)
		N5−H5A···S2#2	153.5
		N5−H5A···S2#3	173.1

[a] Distances are given in Å, angles in degree. Symmetry transformations used to generate equivalent atoms: #1 $-x+1, y, -z+{}^1/_2$; #2 $x, -y+1, z-{}^1/_2$; #3 $x, y-1, z$.

$NH_2)_2$ unit is also present in the hexanuclear complex $[(ZnL)_4(ZnL_2)_2](ClO_4)_4 \cdot 2MeCN$ ($L = SCH_2CH_2NH_2$).[15] The slight structural differences, that is, longer Zn−S and shorter Zn−N bonds than those in **2**, are attributed to the bridging thiolate groups. There is a recent report for a penta coordinate Zn^{II} with N and S donor atoms, but the increase of the coordination number beyond four in that case can be explained by very narrow bite angles of the bipy and the 1,2-benzenedithiolate ligands, providing space for a bridging S atom.[29]

In **3**, one $SCH_2CH_2NH_2$ ligand acts in a N,S chelating mode only, while the other one additionally forms a S−Cd bond to a neighboring molecule (Figure 3a), leading to chains of $Cd(SCH_2CH_2NH_2)_2$ molecules, running along the crystallographic *c* axis (Figure 3b). Hence, each Cd atom is penta coordinated with a $Cd(N_2S_3)$ mode, S2#1 occupying the apex

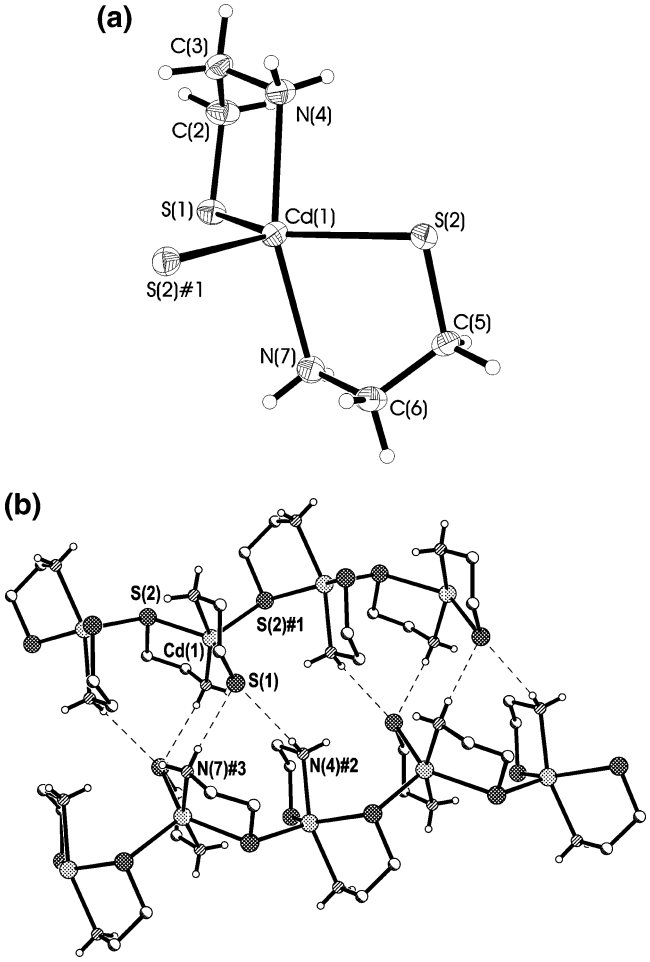

Figure 3. (a) ORTEP diagram of **3** showing the coordination environment at Cd. Displacement ellipsoids are at the 50% probability level. (b) Segment of the crystal structure of **3** showing Cd−S−Cd bridges and hydrogen bonds. Hydrogen atoms bound to carbon atoms are omitted for clarity.

position of a distorted square pyramid. The Cd−S bonds involving bridging S atoms (S2, S2#1) are only slightly longer than those to nonbridging S atoms (S1) (See Table 4). The $[CdS_3]$ unit is planar (Σ S−Cd−S = 360.0°), but the individual angles deviate significantly from 120°. The Cd−S−Cd bridges in **3** are rather short and nearly symmetric, pointing to strong and highly ionic interactions between these atoms. This explains the low solubility of **3** in most solvents except for DMSO. The bigger ionic radius of Cd^{2+} (CN = 4, 0.78 Å; CN = 5, 0.87 Å) compared to that of Zn^{2+} (CN = 4, 0.60 Å; CN = 5, 0.68 Å) and the small amount of energy required to deform the S−Cd−S angle (see Ab initio Geometrical and Thermochemical Studies section further down) are seen as the main reason for the increase of CN_{Cd} from 4 to 5.[30] N−H···S hydrogen bonds occur only to the nonbridging thiolate groups, that is, S1 and its symmetry equivalents. Two of the three hydrogen bonds occur between the chains and hold them together.

Hg displays a bisphenoidal $Hg(N_2S_2)$ coordination mode in **4**, with a nearly linear S−Hg−S arrangement and a narrow N−Hg−N angle (Figure 4a and Table 5). S−Hg−S angles

(29) Hatch, D. M.; Wacholtz, W. F.; Mague, J. T. *Acta Crystallogr., Sect. C* **2003**, *59*, m452−m453.

(30) Shannon, R. D. *Acta Crystallogr., Sect. A* **1976**, *32*, 751−767.

Table 4. Selected Structural Data of **3** from Single Crystal X-ray Diffraction (XRD)[a]

Cd1−S1	2.534(1)	S1−Cd1−S2	140.6(1)	Cd1−S1−C2−C3	−32.1(2)
Cd1−S2	2.620(1)	S1−Cd1−S2#1	113.4(1)	Cd1−S2−C5−C6	−33.4(2)
Cd1−S2#1	2.572(1)	S2−Cd1−S2#1	106.0(1)	S1−C2−C3−N4	59.0(3)
Cd1−N4	2.373(2)	N4−Cd1−N7	160.5(1)	S2−C5−C6−N7	64.0(3)
Cd1−N7	2.382(2)	N4−Cd1−S1	81.2(1)	C2−C3−N4−Cd1	−51.1(3)
S1−C2	1.816(3)	N7−Cd1−S2	78.7(1)	C5−C6−N7−Cd1	−57.9(3)
S2−C5	1.821(3)	Cd1−S1−C2	97.2(1)	C3−N4−Cd1−S1	23.9(2)
C2−C3	1.514(4)	Cd1−S2−C5	97.3(1)	C6−N7−Cd1−S2	27.1(2)
C5−C6	1.517(4)	S1−C2−C3	115.2(2)	N4−Cd1−S1−C2	3.7(2)
C3−N4	1.468(4)	S2−C5−C6	112.4(2)	N7−Cd1−S2−C5	3.2(1)
C6−N7	1.461(4)	C2−C3−N4	111.2(2)	S2−Cd1−S1−C2	−74.0(1)
N4···S1#2	3.518(3)	C5−C6−N7	110.5(2)	S1−Cd1−S2−C5	−86.6(1)
N4···S1#3	3.563(3)	N4−H4A···S1#2	167.2		
N7···S1#4	3.462(3)	N4−H4B···S1#3	147.5		
		N7−H7B···S1#4	174.3		

[a] Distances are given in Å, angles in degrees. Symmetry transformations used to generate equivalent atoms: #1 $x, -y + 1/2, z - 1/2$; #2 $x, -y + 1/2, z + 1/2$; #3 $-x + 1, y - 1/2, -z + 1/2$; #4 $-x + 1, -y + 1, -z + 1$.

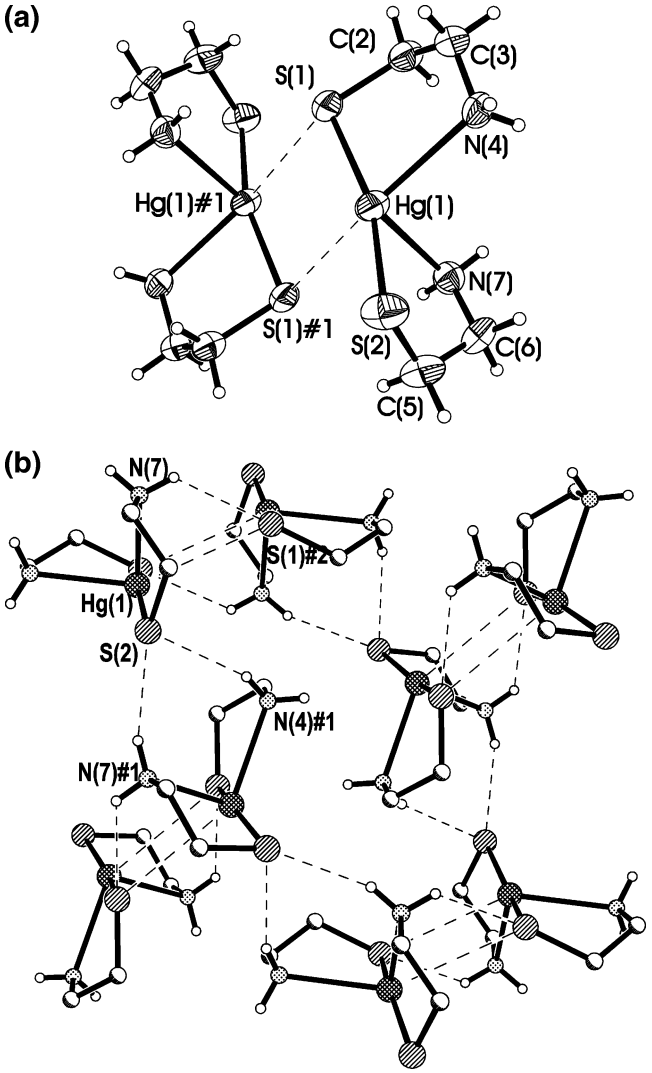

Figure 4. (a) ORTEP diagram of a dimer of **4**. Displacement ellipsoids are at the 50% probability level. (b) Segment of the crystal structure of **4** showing intermolecular hydrogen bonds. Hydrogen atoms bound to carbon atoms are omitted for clarity.

close to 180° are a common feature in Hg^{II} coordination chemistry. Additionally, a long intermolecular Hg···S contact occurs opposite to one Hg−N bond, leading to a weakly bound dimer. The dimers are connected by a net of hydrogen bonds (see Figure 4b). The Hg−S bonds in **4** are only slightly longer than those in $[Hg(HL)_2]Cl_2$, where a two-coordinate Hg atom is present.[20] This is in accordance with the rather long Hg−N bonds in **4**, which obviously have little impact on the HgS_2 geometry.

The hydrogen bonds of all complex molecules, **2**−**4**, are significantly longer than those in **1**, and the N−H···S units deviate more from a linear arrangement than in **1**.

Ab initio Geometrical and Thermochemical Studies. To analyze the coordination modes of **2**, **3**, and **4** in more detail, the molecular structures of the isolated molecules were optimized and thermochemical calculations were performed by means of ab initio methods. The bonds were analyzed in terms of natural bond orbitals (NBOs).[31] The results are summarized in Table 6.

The ab initio bond valences of M−S increase in the order Zn < Cd < Hg, while those of the M−N bonds decrease in this order. The reduction of the M−N bond strength is supported by thermochemical data and an analysis of NBO interactions. For each molecule, a conformer lacking M···N interactions was optimized and its free enthalpy compared to the conformer including M···N interactions. For the former, an anti S−C−C−N conformation was chosen, in which the N atom is far away from the metal. The transformation of the conformer without into the one with M···N interactions becomes more exergonic in the sequence Hg < Cd < Zn; hence, the stability of the M···N interactions increases in the same order. This is reflected by the energies of lp(N)−σ*(M−S) and lp(N)−ry*(M) interactions.

The origin of the preference of Hg^{II} for a linear two-coordination mode has already been controversially discussed in terms of s−p and s−d hybridization.[32] An analysis of the M−S bonds in terms of NBOs revealed a high ionic character, as can be seen from atomic charges and the degree of participation of M orbitals (see Table 6b). The ionic character of the M−S bond increases in the order Hg ≪ Cd < Zn and also with formation of the M−N bond. Concerning the M orbitals which participate in the M−S bonding, only the valence s orbitals seem to contribute significantly. Thus,

(31) Reed, A. E.; Curtiss, L. A.; Weinhold, F. *Chem. Rev.* **1988**, *88*, 899−926.
(32) Wright, J. G.; Natan, M. J.; MacDonnell, F. M.; Ralston, D. M.; O'Halloran, T. V. *Prog. Inorg. Chem. Bioinorg. Chem.* **1990**, *38*, 323−412.

Table 5. Selected Structural Data of **4** from Single Crystal X-ray Diffraction (XRD)[a]

Hg1−S1	2.357(2)	S1−Hg1−S2	161.2(1)	Hg1−S1−C2−C3	−51.0(6)
Hg1−S2	2.364(2)	S1−Hg1···S1#1	87.0(1)	Hg1−S2−C5−C6	43.9(7)
Hg1···S1#1	3.545(2)	S2−Hg1···S1#1	92.8(1)	S1−C2−C3−N4	60.0(8)
Hg1−N4	2.650(6)	N4−Hg1−N7	93.2(2)	S2−C5−C6−N7	−63.9(9)
Hg1−N7	2.531(6)	Hg1−S1−C2	100.5(3)	C2−C3−N4−Hg1	−33.5(7)
S1−C2	1.818(8)	Hg1−S2−C5	99.1(2)	C5−C6−N7−Hg1	44.1(8)
S2−C5	1.814(9)	S1−C2−C3	115.0(6)	C3−N4−Hg1−S1	3.5(4)
C2−C3	1.501(11)	S2−C5−C6	113.7(6)	C6−N7−Hg1−S2	−14.0(5)
C5−C6	1.513(12)	C2−C3−N4	111.5(6)	N4−Hg1−S1−C2	20.6(3)
C3−N4	1.481(9)	C5−C6−N7	111.2(6)	N7−Hg1−S2−C5	−13.5(4)
C6−N7	1.455(10)	N4−H4B···S2#1	158.6	S2−Hg1−S1−C2	139.4(3)
N4#1···S2	3.638(8)	N7−H7A···S1#2	127.0	S1−Hg1−S2−C5	141.7(4)
N7···S1#2	3.455(7)	N7−H7B···S2#1	157.0		
N7#1···S2	3.407(6)				

[a] Distances are given in Å, angles in degrees. Symmetry transformations used to generate equivalent atoms: #1 $x - 1/2$, $-y + 1/2$, $z - 1/2$; #2 $-x + 1$, $-y$, $-z + 1$. Structural parameters of **4** are in good agreement with those mentioned by Fleissner et al. for the same compound.[19]

Table 6. (a) Selected ab initio [MP2/LANL2DZ(d,f)] Structural Parameters (Internuclear Distances in Å, Angles in Degrees) and (b) Thermochemical Data (in kJ mol^{-1}) and Data from a Bond Analysis of M(SCH$_2$CH$_2$NH$_2$)$_2$ (C_2 symmetry, M = Zn, Cd, Hg) with and without Intramolecular M−N Bonds[a]

Part a

	M = Zn	M = Cd	M = Hg
	With M−N Bond		
M1−S1	2.291	2.443	2.436[b]
M1−N5	2.185	2.411	2.591
ν_{MS}[c]	0.572	0.640	0.721
ν_{MN}[c]	0.323	0.294	0.201
S2−M1−S2′	146.1	156.5	168.8
N5−M1−N5′	105.0	103.4	103.4
	Without M−N Bond		
M1−S2	2.194	2.359	2.383
ν_{MS}[c]	0.743	0.803	0.832
S2−M1−S2′	177.5	179.2	179.5

Part b

	M = Zn	M = Cd	M = Hg
	With M−N Bond		
participation of M orbitals in M−S bond	10.3%	11.7%	18.9%
M orbitals participating in M−S bond	$sp^{0.05}d^{0.01}$	$sp^{0.05}d^{0.01}$	$sp^{0.03}d^{0.04}$
q(M)[d]	+1.55	+1.52	+1.32
lp(N)−σ*(M−S)[e]	95.5	54.0	33.9
lp(N)−ry*(M)[e,f]	52.6	15.4	
$\Delta_{donor-acceptor}G^{298}$[g]	−158	−128	−82
$\Delta_{decomposition}G^{298}$[h]	+202	+116	+16
	Without M−N Bond		
participation of M orbitals in M−S bond	16.1%	17.7%	24.9%
M orbitals participating in M−S bond	$sp^{0.03}d^{0.02}$	$sp^{0.03}d^{0.03}$	$sp^{0.02}d^{0.06}$
q(M)[d]	+1.41	+1.36	+1.18

[a] For plots of the ab initio optimized molecular structures, see Figures S2 and S3 in the Supporting Information. [b] The lengths of the Hg−S bonds are only badly described with the MP2/LANL2DZ(d,f) model. Its ab initio optimized value is, on average, 0.085 Å bigger than what is found in the solid state. This mismatch can neither be due to the different structural types—ab initio gives r_e structures and XRD gives r_a structures[60]—nor can it be attributed to strong intermolecular forces in the solid state. [c] ν_{MS} and ν_{MN} are bond valences of the M−S and M−N bonds, respectively, according to O'Keeffe and Brese.[61] [d] Natural atomic charge of M in units of the elemental charge. [e] Energy of interaction of the lone pair at one N atom with NBOs localized at M. [f] "ry" denotes Rydberg orbitals; that is, in the present case (n + 1)s, np, nd, and nf (for Zn) or (n − 1)f (for Cd and Hg). n represents the main quantum number. [g] $\Delta_{donor-acceptor}G^{298} = G^{298}$ (with M−N bond) − G^{298} (without M−N bond). [h] $\Delta_{decomposition}G^{298}$ refers to reaction 2.

we prefer to describe the bonding situation in the S−M−S fragment with a 3c4e bond.

Thiols are named mercaptans as well, since they precipitate Hg^{II} from aqueous solutions. We found that the higher affinity of Hg^{II} for thiolate ligands, compared to Cd^{II} and Zn^{II}, contrasts with the stability of the thiolates. The decomposition of gaseous ML_2 into metal, M, and disulfide, L−L, according to reaction 2 was analyzed by a combination of experimental and ab initio methods (terms in parentheses refer to the state):

$$ML_2\ (gas) \rightarrow M\ (standard) + L{-}L\ (gas) \qquad (2)$$

The reaction can be divided into two steps:

$$ML_2\ (gas) \rightarrow M\ (atom) + L{-}L\ (gas) \qquad (2a)$$

The free enthalpies of eq 2b (Zn = −95, Cd = −77, and

$$M\ (atom) \rightarrow M\ (standard) \qquad (2b)$$

Hg = −33 kJ mol^{-1}) are taken from the literature,[33] while those of eq 2a are calculated with the MP2/LANL2DZ(d,f) model. The data given in Table 6b reveal that ΔG of the decomposition reaction becomes more endergonic in the sequence Hg < Cd < Zn; that is, mercury(II) thiolates are less stable than their cadmium and zinc analogues. The contrast between the high affinity of Hg^{II} for thiolate ligands and the low stability of mercury thiolate complexes toward decomposition to Hg and disulfide can be resolved by considering the standard free enthalpies of Zn_{aq}^{2+} (−147 kJ mol^{-1}), Cd_{aq}^{2+} (−78 kJ mol^{-1}), and Hg_{aq}^{2+} (+164 kJ mol^{-1}).[34] The formation of HgL_2 from an aqueous solution of Hg^{2+} and L^- is very exergonic as a result of the high standard free enthalpy of Hg_{aq}^{2+}, a thermodynamic value not relevant for the stability of HgL_2 with respect to Hg and L−L.

Another interesting trend revealed by ab initio methods is the variation of the energy of ML_2 with the S−M−S angle. The S−M−S angles of all conformers without M···N interactions optimized to values close to 180°, as it is expected from the VSEPR model. For conformers with M···N interactions, a(S−M−S) increases in the order Zn <

(33) Hurtado, I.; Neuschütz, D. *Thermodynamic Properties of Inorganic Materials*; Springer: Berlin, 1999; Vol. 4/19.
(34) Stumm, W.; Morgan, J. J. *Aquatic Chemistry. An Introduction Emphasizing Chemical Equilibria in Natural Waters*; Wiley & Sons: New York, 1981.

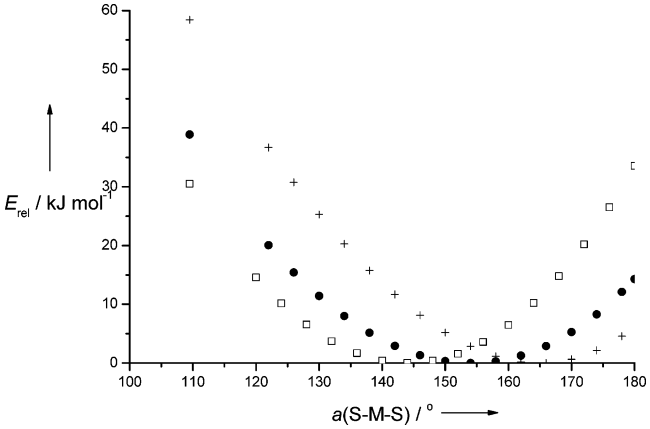

Figure 5. MP2/LANL2DZ(d) relative potential energies as a function of the S−M−S angle of $Zn(SCH_2CH_2NH_2)_2$ (□), $Cd(SCH_2CH_2NH_2)_2$ (●), and $Hg(SCH_2CH_2NH_2)_2$ (+), with respect to their individual minimum energies.

Cd < Hg, and the large S−Hg−S angle found in the solid-state structure of **4** is seen to be much more of a prerequisite for rather than a consequence of the weak intermolecular Hg···S interaction. A plot of the relative energy of $M(SCH_2CH_2NH_2)_2$ (with M···N interactions) against *a*(S−M−S) reveals its pronounced dependence (Figure 5). For M = Hg, where the difference in the strengths of M−S and M−N bonds is largest, the arrangement of the Hg−S bonds dominates the coordination geometry of **4**, leading to a wide S−Hg−S angle. Cd and, even more so, Zn, have a smaller difference between the strengths of their M−S and M−N bonds, and the latter has an increasing influence on the coordination geometry. This is expressed in smaller S−M−S angles. A deformation of *a*(S−Zn−S), *a*(S−Cd−S), and *a*(S−Hg−S) away from their ab initio optimized values to those which they adopt in the solid state (i.e., 127.1° for **2**, 140.6° for **3**, and 161.2° for **4**), needs approximately 7 kJ mol^{-1} for **2**, 4 kJ mol^{-1} for **3**, and virtually no energy for **4**. The differences of *a*(S−M−S) between ab initio and X-ray diffraction analysis (XRD) structures can, thus, easily be rationalized in terms of intermolecular interactions, which are strongest for **3**. If a tetrahedral S−M−S angle is enforced, the energy of **2** raises by 30.5 kJ mol^{-1} above that of the local minimum. For **3** and **4**, energies of 38.9 and 58.4 kJ mol^{-1}, respectively, are necessary to compress S−M−S to a value of 109.47°. This means that a substitution of Zn^{II} by Cd^{II} or Hg^{II} in a $M(N_2S_2)$ environment becomes less favorable, if relatively small S−M−S angles have to be adopted. On the other hand, if the ligand environment is flexible, substitution of Zn^{II} by Cd^{II} or Hg^{II} leads to radial and angular distortions in the N_2S_2 coordination environment.

A survey of complex structures exhibiting $M(S_4)$ or $M(N_2S_2)$ coordination modes (M = Zn, Cd, Hg; from Cambridge Crystallographic Data Centre),[35] as well as an analysis of structurally known zinc-finger proteins within a $Zn(N_2S_2)$ environment (from Protein Data Bank),[36] corroborates the results obtained for the ML_2 complexes. Only $M(S_4)$ complexes with four independent ligands were considered, and 11 $Zn(S_4)$, 18 $Cd(S_4)$, and 29 $Hg(S_4)$ coordination environments were found to fit the selection criteria. Compared to the Zn complexes, the coordination environments of Cd and Hg showed only radial and no angular distortions. The averages of the S−M−S angles are 109.6, 109.5, and 109.2°, respectively, for Zn, Cd, and Hg. A total of 50, 48, and 56% of the angles fall between 105 and 115°, respectively, and except for two cases, where different types of S-donor ligands bind to Hg, no angle was found bigger than 127°. On the other hand, the average M−S distances were found to be 2.349(5) Å for M = Zn, 2.539(11) Å for M = Cd, and 2.559(37) Å for M = Hg, showing a radial distortion from Zn to Cd and Hg. For $M(N_2S_2)$, structures with two N or two S atoms being part of the same ligand were ignored, leaving 80 Zn, 13 Cd, and 10 Hg structures. The average S−M−S angles show marked differences between Zn [122.9(11)°; smallest is 99.8°, largest is 142.3°] and Cd [124.1(28)°; smallest is 101.9, largest is 139.1°] on one side and Hg [152.8(29)°, smallest is 134.9, largest is 164.8°] on the other (values in parentheses represent standard errors). That is, Hg^{II} but not Cd^{II} introduces a large angular distortion compared to Zn^{II}. Thus, a substitution of Zn^{II} for Cd^{II} or Hg^{II} has different structural impacts for $M(S_4)$ and $M(N_2S_2)$ coordination environments. A survey of 17 single-crystal X-ray structures of zinc-finger proteins, containing, altogether, 65 Zn atoms in a $Zn(N_2S_2)$ coordination mode, gave the following results: The average S−Zn−S angle is 112.3(13)°, the smallest and the largest values being 83.7 and 142.0°, respectively, and 63% of all S−Zn−S angles fall within 110 and 120°. Thus, the protein environment enforces, on average, significantly smaller S−Zn−S angles than those found in complexes with small N,S ligands. According to the ab initio results presented, this means that Zn^{2+} is better protected against substitution by Cd^{2+} or Hg^{2+} in a zinc-finger protein than in a small molecular complex which does not provide such a rigid coordination environment.

IR and NMR Spectra of 2−4. Since **3** lacks any molecular symmetry in the solid state, its IR spectrum contains more bands than that of **2**. Complex **4** does not have any molecular symmetry in the solid state either, but the structural difference between its two ligands is small; thus, its IR spectrum displays less bands than that of **3**. Complexes **2**−**4** exhibit a smaller $\nu(NH_2)$ than $H_3CSCH_2CH_2NH_2$ (3380 cm^{-1}) does.[37] The shift of $\nu(NH_2)$ to lower wavenumbers on coordination of a primary amine to a metal ion is well-known.[38] $\nu(NH_2)$ is smallest for **2**, where the M···N interaction is strongest, in accordance with results from single-crystal XRD and ab initio calculations. ν_{as}(M−S) could be assigned with the support of MP2/LANL2DZ(d) frequencies for M = Zn and Hg. ν_{as}(Hg−S) is within the range (256−405 cm^{-1}) found for other mercury(II) thiolates with a nearly linear S−Hg−S fragment.[32] It occurs at a

(35) Allen, F. H. *Acta Crystallogr., Sect. B* **2002**, *58*, 380−388.
(36) Berman, H. M.; Westbrook, J.; Feng, Z.; Gilliland, G.; Bhat, T. N.; Weissig, H.; Shindyalov, I. N.; Bourne, P. E. *Nucleic Acids Res.* **2000**, *28*, 235−242.
(37) Jinachitra, S.; MacLeod, A. J. *Tetrahedron* **1979**, *35*, 1315−1316.
(38) Sen, D. N.; Mizushima, S.-I.; Curran, C.; Quagliano, J. V. *J. Am. Chem. Soc.* **1955**, *77*, 211−212.

Table 7. ^{113}Cd and ^{199}Hg NMR Data of **3**, **4**, and $[Hg(HL)_2]Cl_2$[a]

compound	csa[b]	η[c]	σ_{iso}	σ_{11}	σ_{22}	σ_{33}	δ_{sol}
3	−345	1.22	669	924	644	439	-[d]
4	−2497	0.55	−633	657	−258	−2298	−551
$[Hg(HL)_2]Cl_2$	−2681	0.70	−1018	501	−750	−2805	−659

[a] All solution NMR spectra were recorded in a DMSO-d_6 solution. Shielding parameters were obtained by fitting the experimental spectra with the "dmfit" program.[62] [b] Chemical shift anisotropy. csa = $\sigma_{33} - (\sigma_{11} + \sigma_{22})/2$. [c] $\eta = (\sigma_{22} - \sigma_{11})/(\sigma_{33} - \sigma_{iso})$. [d] No ^{113}Cd spectrum of **3** could be obtained as a result of its low solubility.

significantly higher frequency than ν_{as}(Zn−S), demonstrating the higher covalent character of the Hg−S bond compared to that of the Zn−S bond.

The ^{199}Hg NMR shift proved suitable to distinguish between three- and four-coordinate Hg^{II} since a low-field shift was observed with increasing coordination number.[32,39] We investigated solution and solid-state CPMAS ^{113}Cd and ^{199}Hg NMR spectra of **3**, $[Hg(HL)_2]Cl_2$, and **4** (Table 7). The isotropic ^{113}Cd NMR shift of **3** in the solid state is low-field shifted compared to the shift of $[Cd(SR)_2(N\text{-donor})_2]$ complexes (372−492 ppm),[40] a fact attributed to the higher coordination number of the Cd atom in **3**. The ^{199}Hg CPMAS spectra of $[Hg(HL)_2]Cl_2$ and **4** exhibit extended ($N > 10$) spinning sidebands, even at spinning rates as high as 7000 Hz. Consequently, very large chemical shift anisotropies (csa) were found. σ_{iso} of $[Hg(HL)_2]Cl_2$ ($CN_{Hg} = 2$) is shifted nearly 400 ppm to high field relative to that of **4** ($CN_{Hg} = 4$). Our results, thus, corroborate the above-mentioned high-field shift of $\delta(^{199}Hg)$ with decreasing coordination number.

Conclusion

Dipolar forces and hydrogen bonds favor the zwitterionic form of cysteamine, $^-SCH_2CH_2NH_3^+$, over the nonzwitterionic tautomer, $HSCH_2CH_2NH_2$, in aqueous solution and in the solid state. Cysteaminate $^-SCH_2CH_2NH_2$ (= L^-) as a relatively small chelating N,S ligand allows Zn^{II}, Cd^{II}, and Hg^{II} to show intrinsic features of their coordination chemistry in the homoleptic ML_2 complexes. The M−S bonds in these complexes have a high ionic character, and the S−M−S unit is best described by a 3c4e bond. Apart from the size of the M^{II} ions, the preferred S−M−S angles in mononuclear ML_2 and the energy necessary for their distortion are seen to be the factors ruling the coordination modes in these complexes. A relatively narrow S−Zn−S angle renders a substitution of Zn^{II} by Cd^{II} or Hg^{II} from a $Zn(N_2S_2)$ environment unfavorable.

Experimental Section

General Procedures. Metal salts and cysteamine hydrochloride, $[H_2L]Cl$, were used as purchased. Solvents were purified according to standard procedures. HL,[41] ZnL_2,[42] and $[Hg(HL)_2]Cl_2$[20] were prepared according to literature procedures. Solution NMR: Bruker DRX 400, $B_1(^1H) = 400.0$, $B_1(^{13}C) = 100.577$, $B_1(^{14}N) = 28.9$, $B_1(^{199}Hg) = 71.619$ MHz. Standards: TMS (^{1}H, ^{13}C), $NH_{3,l}$ (^{14}N), and $Hg(CH_3)_2$ (^{199}Hg). Solid-state NMR: Bruker DSX 400, $B_1(^{113}Cd) = 88.742$, $B_1(^{199}Hg) = 71.571$ MHz. Standards: $Cd(NO_3)_2 \cdot 4H_2O$ (^{113}Cd) and $Hg(O_2CCH_3)_2$ (^{199}Hg). IR: Mattson Galaxy 2030 FTIR, resolution 4 cm^{-1}, CsI pellets, range 4000−200 cm^{-1}. Raman spectroscopy: Bruker RFS 100, excitation with $\lambda = 1064$ nm. The CHNS analysis was performed with an Elemental Vario EL2.

Zinc bis(2-Aminoethanethiolate), ZnL_2, 2. Single crystals of **2** suitable for X-ray diffraction were obtained from a saturated solution of **2** in ethanol on cooling from room temperature to 5 °C. Elem Anal. Calcd (%) for $C_4H_{12}N_2S_2Zn$ (217.67): C, 22.07; H, 5.56; N, 12.87; S, 29.46. Found: C, 21.85; H, 5.87; N, 12.63; S, 29.23. ^{1}H NMR (D_2O): 2.69 [t, ^3J(H,H) = 5.8 Hz, 2H, NCH_2], 2.48 [t, ^3J(H,H) = 5.8 Hz, 2H, SCH_2]. IR (CsI): 3228 [vs, $\nu(NH_2)$], 3185 [s, $\nu(NH_2)$], 3100 [vs, $\nu(NH_2)$], 2950 [m, $\nu_{as}(CH_2)$], 2915 [s, $\nu_{as}(CH_2)$], 2857 [s, $\nu_{as}(CH_2)$], 2838 [m, $\nu_s(CH_2)$], 1581 [s, $\delta(NH_2)$], 1460 [m, $\delta(CH_2)$], 1433 [m, $\delta(CH_2)$], 1386 [w, $\delta(CH_2)$], 1308 [m, $\delta_{tw}(CH_2)$], 1284 [m, $\delta_{tw}(NH_2)$], 1231 [m, $\delta_{tw}(CH_2)$], 1117 [s, $\delta_{tw}(NH_2)$], 1048 [s, ν(N−C)], 986 [m, $\rho(CH_2)$], 921 [w, $\rho(CH_2)$], 838 (m), 669 [m, ν(S−C)], 632 (m), 486 (m), 408 (m), 311 [m, ν_{as}(Zn−S)], 278 cm^{-1} (m).

Preparation of Cadmium bis(2-Aminoethanethiolate), CdL_2, 3. 2-Mercaptoethylammonium chloride, $[H_2L]Cl$ (1.09 g, 9.6 mmol), and sodium hydroxide, NaOH (0.76, 19.0 mmol), were dissolved in 20 mL of methanol, and the precipitated NaCl was filtered off. The filtrate was slowly added to a solution of cadmium acetate dihydrate, $Cd(O_2CCH_3)_2 \cdot 2H_2O$ (1.26 g, 4.7 mmol), in 20 mL of methanol, and the solution was heated to reflux for 30 min. The addition of 5 mL of H_2O to the solution at room temperature led to the precipitation of a colorless solid, which was washed with H_2O and cold methanol and subsequently dried in vacuo. Yield: 0.78 g (62.5%). mp 166 °C. Crystals suitable for X-ray diffraction were obtained by slowly cooling a saturated solution of **3** in DMSO from 100 °C to room temperature. Elem Anal. Calcd (%) for $C_4H_{12}N_2S_2Cd$ (264.69): C, 18.15; H, 4.57; N, 10.59; S, 24.22. Found: C, 18.41; H, 5.15; N, 10.32; S, 24.46. ^{1}H NMR (DMSO-d_6): 3.27 (s, 2H, NH_2), 2.62 (broad m, 2H, NCH_2), 2.45 (broad m, 2H, SCH_2). $^{13}C\{^1H\}$ NMR (DMSO-d_6): 44.4 (NCH_2), 28.6 (SCH_2). IR: 3361 [s, $\nu(NH_2)$], 3304 [vs, $\nu(NH_2)$], 3207 [vs, $\nu(NH_2)$], 3129 [s, $\nu(NH_2)$], 2947 [sh, $\nu(CH_2)$], 2937 [m, $\nu(CH_2)$], 2919 [s, $\nu(CH_2)$], 2906 [s, $\nu(CH_2)$], 2866 [m, $\nu(CH_2)$], 2843 [s, $\nu(CH_2)$], 1598 [s, $\delta(NH_2)$], 1458 [m, $\delta(CH_2)$], 1424 [m, $\delta(CH_2)$], 1381 [m, $\delta(CH_2)$], 1363 [m, $\delta(CH_2)$], 1301 [m, $\delta_{tw}(CH_2)$], 1274 [m, $\delta_{tw}(NH_2)$], 1235 [w, $\delta_{tw}(CH_2)$], 1225 [w, $\delta_{tw}(CH_2)$], 1117 (w), 1097 (w), 1022 [vs, ν(N−C)], 964 [s, ν(N−C)], 914 [s, $\rho(CH_2)$], 832 (m), 667 [m, ν(S−C)], 613 (sh), 589 (m), 528 (m), 457(m), 326 (m), 279 (m), 232 cm^{-1} (s).

Preparation of Mercury bis(2-Aminoethanethiolate), HgL_2, 4. 2-Mercaptoethylammonium chloride, $[H_2L]Cl$ (2.60 g, 22.9 mmol), and sodium hydroxide, NaOH (1.90, 47.5 mmol), were dissolved in 30 mL of methanol, and the precipitated NaCl was filtered off. The filtrate was slowly added to a solution of mercury(II) chloride, $HgCl_2$ (2.76 g, 10.2 mmol), in 60 mL of methanol. A white precipitate which was formed in the initial stage of the reaction vanished when approximately $^2/_3$ of the solution was added. From this solution, the product precipitated at −20 °C as colorless needles. Yield: 2.52 g (85.8%). Single crystals of **4** suitable for X-ray diffraction were obtained from the precipitate. mp 87 °C. Elem Anal. Calcd for $C_4H_{12}N_2S_2Hg$ (352.87): C, 13.62; H, 3.43; N, 7.94; S, 18.17. Found: C, 13.53; H, 3.02; N, 7.91; S, 18.05. ^{1}H NMR (CD_3OD): 2.92 [t, ^3J(H,H) = 3.1 Hz, 2H, NCH_2], 2.83

(39) Natan, M. J.; Millikan, C. F.; Wright, J. G.; O'Halloran, T. V. *J. Am. Chem. Soc.* **1990**, *112*, 3255−3257.
(40) Santos, R. A.; Gruff, E. S.; Koch, S. A.; Harbison, G. S. *J. Am. Chem. Soc.* **1990**, *112*, 9257−9263.
(41) Gabriel, S.; Colman, J. *Chem. Ber.* **1912**, *45*, 1643−1654.
(42) Wragg, R. T. *J. Chem. Soc., C* **1969**, 2087−2092.

Table 8. Crystal Data for Compounds **1**−**4**

	1	**2**	**3**	**4**
empirical formula	C_2H_7NS	$C_4H_{12}N_2S_2Zn$	$C_4H_{12}N_2S_2Cd$	$C_4H_{12}N_2S_2Hg$
FW/g mol^{-1}	77.15	217.67	264.70	352.87
cryst syst	monoclinic	monoclinic	monoclinic	monoclinic
space group	*Cc*	*C*2/*c*	*P*2$_1$/*c*	*P*2$_1$/*n*
Z	4	4	4	4
λ/Å	1.541 78	1.541 78	0.710 73	0.710 73
temp/K	193	295	193	203
ρ_{calcd}/g cm^{-3}	1.221	1.665	2.126	2.691
μ/mm^{-1}	5.08[a]	7.81[b]	3.066[c]	18.07[c]
F(000)	168	448	520	648
cryst size/mm^3	0.32 × 0.51 × 0.58	0.08 × 0.14 × 0.39	0.11 × 0.14 × 0.33	0.17 × 0.36 × 0.80
θ range	$1.5 \le \theta \le 74$	$2 \le \theta \le 74$	$2 \le \theta \le 28.3$	$3 \le \theta \le 28.3$
limiting indices	$-6 \le h \le 6$	$0 \le h \le 22$	$-12 \le h \le 12$	$-12 \le h \le 12$
	$-11 \le k \le 11$	$0 \le k \le 6$	$-15 \le k \le 15$	$-11 \le k \le 12$
	$-10 \le l \le 10$	$-12 \le l \le 12$	$-10 \le l \le 11$	$-14 \le l \le 13$
a/Å	5.1870(4)	18.2166(15)	9.083(1)	9.7018(2)
b/Å	9.3113(8)	4.9242(3)	11.953(2)	9.1374(2)
c/Å	8.847(6)	10.0513(8)	8.284(1)	10.5649(2)
β/deg	100.81(4)	105.647(4)	113.141(2)	111.5621(14)
V/Å^3	419.7(4)	868.2(1)	827.1(3)	871.03(3)
reflns measured	992	1022	9739	10 005
unique reflns	832	882	2017	2166
refln $\|F\| > 4\sigma$(F)	832	854	1721	2009
R [$\|F\| > 4\sigma(F)$][d]	0.0513	0.0328	0.0294	0.0411
GOF on F^2	1.250	1.156	1.027	1.155
largest diff. peak and hole *e* Å^{-3}	0.41/−0.38	0.54/−0.54	0.85/−1.27	1.76/−1.26

[a] Absorption correction with ψ scans.[63] [b] Numerical absorption correction.[64] [c] Absorption correction with MULABS.[65] The crystal of **4** was covered and protected by inert oil, which concealed its faces such that they could not be used for a numerical absorption correction. The high redundancy of the reflections measured should ensure a reasonable absorption correction. [d] $R = \Sigma\ ||F_o| - |F_c||/\Sigma\ |F_o|$.

[t, ^3J(H,H) = 3.1 Hz, 2H, SCH_2]. $^{13}C\{^1H\}$ NMR (CD_3OD): 46.1 (NCH_2), 33.0 (SCH_2). $^{199}Hg\{^1H\}$ NMR (CD_3OD): −608.3. $^{199}Hg\{^1H\}$ NMR (DMSO-d_6): −550.6. IR: 3354 [vs, $\nu(NH_2)$], 3282 [s, $\nu(NH_2)$], 3260 [m, $\nu(NH_2)$], 2941 [s, $\nu(CH_2)$], 2904 [s, $\nu_{as}(CH_2)$], 2843 [s, $\nu_{as}(CH_2)$], 2817 [m, $\nu(CH_2)$], 1576 [s, $\delta(NH_2)$], 1448 [m, $\delta(CH_2)$], 1418 [m, $\delta(CH_2)$], 1373 [m, $\delta(CH_2)$], 1300 [m, $\delta_{tw}(CH_2)$], 1271 [s, $\delta_{tw}(CH_2)$], 1215 [m, $\delta_{tw}(CH_2)$], 1065 (m), 938 (m), 888 [vs, δ(N−C)], 826 (s), 661 [m, ν(S−C)], 514 (m), 423 (s), 362 cm^{-1} [s, ν_{as}(Hg−S)].

Crystal Structure Determination. Diffraction experiments were performed on a Turbo CAD4 (Nonius) diffractometer for **1** and **2** and on a SMART CCD (Bruker Nonius) diffractometer for **3** and **4** (diameter of collimator: 0.8 mm). The crystal structures were solved by direct methods and the difference Fourier technique (SIR-92);[43] the structural refinement was against F^2 (SHELXL-97).[44] Hydrogen atoms were localized by difference Fourier maps and refined with a riding model. For **1**, positions of all hydrogen atoms were refined. For **2** and **4**, C−H and N−H distances were fixed; for **3**, C−H distances were fixed, while N−H vector lengths were refined. Details of the crystal structure determinations of **1**−**4** and their crystal data are given in Table 8.

Theoretical Methods. The ab initio calculations were performed using the GAUSSIAN98 software package.[45] For complexes ML_2 (M = Zn, Cd, Hg), geometry optimizations, calculations of vibrational frequencies, and analyses of electronic structures in terms of natural orbitals[31] were performed with second-order Møller−Plesset perturbation theory (MP2) and effective core double-ζ valence basis sets designated either as LANL2DZ(d) or LANL2DZ(d,f). In these basis sets, relativistic effective core potentials and the corresponding double-ζ valence basis sets for S, Zn, Cd, and Hg,[46,47] augmented by an appropriate d-type function for S and, in the latter case, also by f-type polarization functions for Zn, Cd, and Hg (with exponents according to Höllwarth et al.),[48] were used. For C and N, Dunning's and Hay's [3s2p] contracted valence double-ζ basis,[49] augmented with a set of d-type polarization functions (exponent 0.75 for C and 0.80 for N) was used. For H, Huzinaga's (4s) basis contracted to [2s] was used.[50] For all molecules ML_2 investigated, C_2 symmetry was enforced. Assignments of experimental vibrational frequencies were supported by ab initio calculated wavenumbers and intensities. Geometry optimizations, single-point energies, and the calculation of vibrational frequencies of isolated $^-SCH_2CH_2NH_3^+$ and $HSCH_2CH_2NH_2$ were performed with the G2 method.[51] Starting geometries were based on single-crystal X-ray and gas-phase structures,[11] respectively. For

(43) Altomare, A.; Cascarano, G.; Giacovazzo, C.; Guagliardi, A.; Burla, M. C.; Polidori, G.; Camalli, M. *J. Appl. Crystallogr.* **1994**, *27*, 435−436.
(44) Sheldrick, G. M. *SHELXL-97, Program for Crystal Structure Refinement*; University of Göttingen: Göttingen, Germany, 1997.
(45) Frisch, M. J.; Trucks, G. W.; Schlegel, H. B.; Scuseria, G. E.; Robb, M. A.; Cheeseman, J. R.; Zakrzewski, V. G.; J. A. Montgomery, Jr.; Stratmann, R. E.; Burant, J. C.; Dapprich, S.; Millam, J. M.; Daniels, A. D.; Kudin, K. N.; Strain, M. C.; Farkas, O.; Tomasi, J.; Barone, V.; Cossi, M.; Cammi, R.; Mennucci, B.; Pomelli, C.; Adamo, C.; Clifford, S.; Ochterski, J.; Petersson, G. A.; Ayala, P. Y.; Cui, Q.; Morokuma, K.; Malick, D. K.; Rabuck, A. D.; Raghavachari, K.; Foresman, J. B.; Cioslowski, J.; Ortiz, J. V.; Baboul, A. G.; Stefanov, B. B.; Liu, G.; Liashenko, A.; Piskorz, P.; Komaromi, I.; Gomperts, R.; Martin, R. L.; Fox, D. J.; Keith, T.; Al-Laham, M. A.; Peng, C. Y.; Nanayakkara, A.; Gonzalez, C.; Challacombe, M.; Gill, P. M. W.; Johnson, B.; Chen, W.; Wong, M. W.; Andres, J. L.; Gonzalez, C.; Head-Gordon, M.; Replogle, E. S.; Pople, J. A. *GAUSSIAN 98*, revision A.7; Gaussian, Inc.: Pittsburgh, PA, 1998.
(46) Dunning, T. H. *J. Chem. Phys.* **1971**, *55*, 716−723.
(47) Dunning, T. H. *J. Chem. Phys.* **1970**, *53*, 2823−2833.
(48) Höllwarth, A.; Böhme, M.; Dapprich, S.; Ehlers, A. W.; Gobbi, A.; Jonas, V.; Köhler, K. F.; Stegmann, R.; Veldkamp, A.; Frenking, G. *Chem. Phys. Lett.* **1993**, *208*, 237−240.
(49) Dunning, T. H.; Hay, P. J. In *Modern Theoretical Chemistry*; Schaefer, H. F., Ed.; Plenum Press: New York, 1977; Vol. 4, pp 1−27.
(50) McLean, A. D.; Chandler, G. S. *J. Chem. Phys.* **1980**, *72*, 5639−5648.
(51) Curtiss, L. A.; Raghavachari, K.; Trucks, G. W.; Pople, J. A. *J. Chem. Phys.* **1991**, *94*, 7221−7230.

investigations using the Onsager reaction field model,[52−54] molecular geometries were optimized at the HF/6-31G(d) level and, subsequently, MP2/6−31(d)//HF/6-31G(d) single-point energy calculations were performed. The radius of the cavity in the Onsager model was calculated as 0.3242 nm, using the density obtained from the single-crystal XRD experiment.

Acknowledgment. This paper is dedicated to Prof. Dr. Martin Dräger on the occasion of his 65th birthday.

Supporting Information Available: Selected graphic plots, Cartesian coordinates, and energies of all ab initio optimized structures. Details about the X-ray crystal structures, including tables of crystal data and structure refinement, atomic coordinates, bond lengths and angles, and anisotropic displacement parameters for **1**−**4** (in CIF format). This material is available free of charge via the Internet at http://pubs.acs.org.

IC050814M

(52) Onsager, L. *J. Am. Chem. Soc.* **1936**, *58*, 1486−1493.
(53) Wong, M. W.; Frisch, M. J.; Wiberg, K. B. *J. Am. Chem. Soc.* **1991**, *113*, 4776−4782.
(54) Wong, M. W.; Wiberg, K. B.; Frisch, M. J. *J. Am. Chem. Soc.* **1992**, *114*, 1645−1652.
(55) Prey, V.; Unger, W. *Liebigs Ann. Chem.* **1962**, *651*, 154−161.
(56) Reitmeier, R. E.; Sivertz, V.; Tartar, H. V. *J. Am. Chem. Soc.* **1940**, *62*, 1943−1944.
(57) Davis, R. E.; Molnar, S. P.; Nehring, R. *J. Am. Chem. Soc.* **1969**, *91*, 97−103.
(58) Gallaugher, A. F.; Hibbert, H. *J. Am. Chem. Soc.* **1936**, *58*, 813−816.
(59) Thalladi, V. R.; Boese, R.; Weiss, H.-C. *J. Am. Chem. Soc.* **2000**, *122*, 1186−1190.
(60) Kuchitsu, K. *Accurate Molecular Structures*; Domenicano, A., Hargittai, I., Eds.; Oxford University Press: Oxford, U. K., 1992.
(61) O'Keeffe, M.; Brese, N. E. *J. Am. Chem. Soc.* **1991**, *113*, 3226−3229.
(62) Massiot, D.; Fayon, F.; Capron, M.; King, I.; Le Calve, S.; Alonso, B.; Durand, J.-O.; Bujoli, B.; Gan, Z.; Hoatson, G. *Magn. Reson. Chem.* **2002**, *40*, 70−72.
(63) Draeger, M.; Gattow, G. *Acta Chem. Scand.* **1971**, *25*, 761−762.
(64) Meulenaer, J. D.; Tompa, H. *Acta Crystallogr.* **1965**, *19*, 1014−1018.
(65) Blessing, R. *Acta Crystallogr., Sect. A* **1995**, *51*, 33−38.